Journal of the Korean Ceramic Society
Vol. 43, No. 1, pp. 4~9, 2006.

Effects of the Loading Rate and Humidity in the Fracture Toughness Testing of Alumina

Seong-Jai Cho,† Jai-Chun Kim, Kyung-Jin Yoon, Min-Cheol Chu, Yoon-Cheol Lee, George Quinn,* and Hong-Lim Lee**

Division of Chemical Metrology and Materials Evaluation, Korea Research Institute of Standards and Science, Daejeon 305-600, Korea
**Ceramics Division, National Institute of Standards and Technology, Gaithersburg, MD 20899, U.S.A.*
***Department of Ceramic Engineering, Yonsei University, Seoul 120-749, Korea*
(Received October 25, 2005; Accepted November 10, 2005)

ABSTRACT

To test the fracture toughness of alumina, a Surface-Crack-in-Flexure (SCF) method, a Single-Edge-Precracked-Beam (SEPB) method and a Single-Edge-V-Notched-Beam (SEVNB) method were used at crosshead rates ranging from 0.005 mm/min to 2 mm/min and relative humidity ranging from 15% to 80%. The results show that the fracture toughness tested by the SCF method increases with either an increasing loading rate or decreasing relative humidity; in contrast, the toughness by the SEPB method and the SEVNB method does not depend on the loading rate or the relative humidity. Theoretical analysis of the way slow crack growth affects the apparent fracture toughness indicates that the three testing methods have different effects with respect to the loading rate and the relative humidity; moreover, these differences are attributable to differences in the size of the cracks or notches.

Key words*: *Fracture toughness, Alumina, Relative humidity, Loading rate, Slow crack growth

1. Introduction

The strength of some oxide ceramics or oxide-containing ceramics is known to decrease as the loading rate decreases.[1-5] Some authors have reported that the strength also decreases as the relative humidity increases.[6-8] The effects of the loading rate and humidity on strength are associated with Slow Crack Growth (SCG) during testing. As the loading rate decreases, the period of SCG increases, leading to a decrease in strength. As the relative humidity increases, the rate of SCG increases; and these increases also lead to a decrease in strength.

Many methods are used to test the fracture toughness of ceramics. Most methods, however, commonly involve a procedure of testing the fracture stress of previously cracked or notched specimens. Because cracks or notches are expected to grow slowly during fracture stress testing, the loading rate and relative humidity may affect the values measured in fracture toughness testing, as they do in strength testing. However, few investigations have explored this topic.[9,10] As a result, the effects of the loading rate and humidity in fracture toughness testing are not clearly understood yet.

Our purpose therefore is to investigate the effects of the loading rate and relative humidity in the following three methods of fracture toughness testing: the Surface-Crack-in-Flexure (SCF) method,[11] the Single-Edge-Precracked-Beam (SEPB) method,[12] and the Single-Edge-V-Notched-Beam (SEVNB) method.[9] Alumina, which is prone to SCG, was chosen as a model material for our experiments. The experimental results show that the loading rate and relative humidity significantly influence the measured data in the SCF method but not the data in the SEPB method and the SEVNB method. To provide a theoretical basis for these experimental results, we considered the size of the cracks or notches when we analyzed how the loading rate and humidity affected the fracture toughness.

†Corresponding author : Seong-Jai Cho
E-mail : sjcho@kriss.re.kr
Tel : +82-42-868-5388 Fax : +82-42-868-5032

2. Experimental Procedure

Alumina of 99.5% purity (AD995, Coors Tek, South Korea) was received in plate form, 10 × 10 × 1 cm. Fig. 1 shows the microstructure of the material. Some pores were present, and the grain size ranged from 2 μm to 5 μm. We cut and ground the material plates into bar specimens of 3 × 4 × 40 mm, and then chamfered about 0.12 mm of the specimen edges. Machined from several plates, the specimens were randomized to avoid plate-to-plate variation.

After introducing cracks or notches on the 3 × 40 mm surfaces of specimens, we used Knoop indentation at 49 N to introduce surface cracks for the SCF method. During the indentation, we tilted the specimens 0.5° from the loading

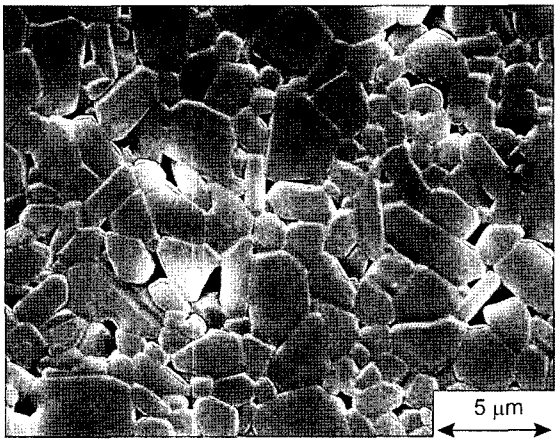

Fig. 1. Microstructure of the alumina used in the experiments.

axis to facilitate the later detection of the cracks on the fractured surfaces.[11] Some of the surface material was polished away to remove the residual stress that had been produced by the indentation. The half-widths of the cracks ranged from 70 μm to 150 μm.

Using a V-shaped thin diamond wheel, we machined the notches for the SEVNB method to a depth of about 1.2 mm. We then sharpened the notch tips further by polishing away 0.2 mm to 0.4 mm with a razor blade sprinkled with 1 μm diamond particles. The radii of the notch roots were less than 10 μm. The cracks for the SEPB method were introduced by bridge-loading specimens that had already been Vickers-indented at 98 N. To help us determine the size of the cracks on the fractured surfaces, we used a dye that penetrated into the cracks. The depth of the cracks was 1.6 mm to 2.1 mm.

To measure the fracture stress of the specimens, we used a four-point flexure method in a humidity/temperature chamber. The fixture had an outer span of 30 mm and an inner span of 10 mm. In addition, to investigate the effect of the loading rate, we used fracture stress testing at crosshead rates that varied from 0.005 mm/min to 2 mm/min at a constant relative humidity of 60%. We also investigated the effect of humidity by varying the relative humidity from 15% to 80% at a crosshead rate of 0.5 mm/min. Fracture stress testing was also conducted under an inert condition. For this purpose, the specimens were coated with liquid paraffin and then tested in a nitrogen gas atmosphere at a crosshead rate of 0.5 mm/min.[13] We conducted the entire fracture stress testing at 22°C.

When examining the fractured surfaces, we used an optical microscope to assess the validity and determine the size of the cracks or notches, especially for the SEPB specimens. The validity of the cracks for the SEPB specimens was assessed in accordance with a relevant standard.[14] We then calculated the fracture toughness from the fracture stress and from the size of the cracks or notches. A minimum of five valid items of data was used to average the fracture toughness under each condition.

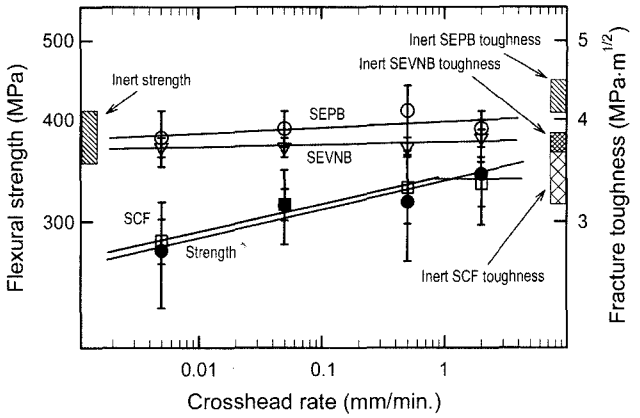

Fig. 2. Change of flexural strength and fracture toughness as a function of the crosshead rate. The bars for the data points represent standard deviations.

3. Results

Fig. 2 presents the change of fracture toughness as a function of the crosshead rate. We also tested the flexural strength, the results of which are presented in Fig. 2 for comparison. The strength and toughness values that were tested under an inert condition are presented as blocks in the vertical axes. The flexural strength clearly increased as the crosshead rate increased. In addition, the fracture toughness as determined by the SCF method also increased as the crosshead rate increased. The toughness eventually neared an inert value at a crosshead rate of 2 mm/min. In contrast, the fracture toughness values that were determined by the SEPB method and the SEVNB method were close to corresponding inert values and did not change with the crosshead rate.

Fig. 3 presents the change of fracture toughness and flexural strength as a function of relative humidity. Until the relative humidity increased to 40%, the fracture toughness by SCF method did not change with the relative humidity and was close to an inert value. However, as the humidity

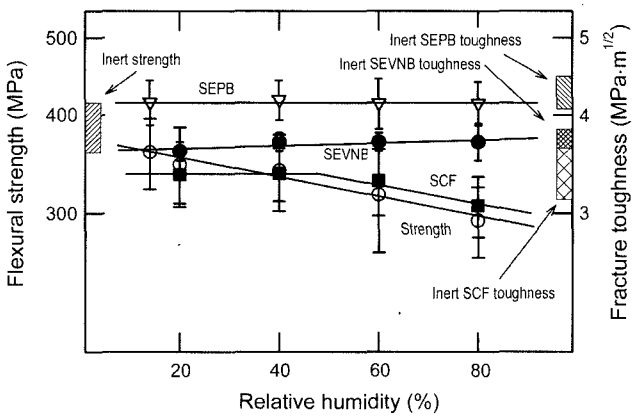

Fig. 3. Change of flexural strength and fracture toughness as a function of the relative humidity. The crosshead rate was 0.5 mm/min for all tests.

increased further, the toughness decreased. In contrast, the fracture toughness values that were determined by the SEPB method and the SEVNB method were close to corresponding inert values and did not change with the humidity. As previously reported, the flexural strength decreased as the relative humidity increased.[8,13]

Figs. 2 and 3 show that the values of the inert fracture toughness depend on the testing method. The inert toughness increases in the order of the testing methods: namely, the SCF method, the SEVNB method and the SEPB method. The R-curve behavior of the alumina may explain why the level of toughness is higher in the SEPB method than in the SCF method. Ceramics that exhibit R-curve behavior manifest the following principle: the larger the crack size, the larger the fracture toughness. Note also that the crack size in the SEPB specimens is significantly larger than the crack size in the SCF specimens. Moreover, the level of toughness is lower in the SEVNB method than in the SEPB method, most likely because the wake of the crack lacks a toughening mechanism, such as grain bridging.

4. Theoretical Analysis

The experimental results show that the effect of the loading rate and relative humidity is significant in the SCF method of testing fracture toughness, whereas the effect is negligible in the SEPB and SEVNB methods of testing fracture toughness. The effect of the loading rate and relative humidity may depend on the size of the crack or notch (for convenience, we refer to both the crack and the notch simply as 'crack').

When cracks are relatively short, even a small amount of SCG crack extension can significantly reduce the fracture stress. Thus, the effect of the loading rate and humidity in fracture toughness testing can be large. When cracks are relatively long, however, the SCG crack extension, which is small in comparison to the crack size, may not significantly affect the fracture stress. As a result, the loading rate and humidity may have a negligible effect on the toughness testing. We therefore considered crack size in our theoretical analysis of the way the loading rate and humidity affect fracture toughness.

We started our analysis with the following fracture mechanics equation:

$$K_{IC} = Y\sigma_f c_f^{1/2} = Y\sigma_f(c_o+\Delta c)^{1/2} \tag{1}$$

where K_{IC} is the material-inherent, environment-insensitive fracture toughness of the ceramics; Y is crack geometrical factor; σ_f is the fracture stress; c_f is the crack size at the fracture; c_o is the initial crack size; and Δc is the crack extension by the SCG method ($= c_f - c_o$). We assumed that K_{IC} does not change with the crack size (that is, no R-curve behavior). We also assumed that Y does not change with the crack extension by the SCG method. We can obtain K_{IC} by testing under an inert condition where no SCG occurs ($\Delta c = 0$):

$$K_{IC} = Y\sigma_o c_o^{1/2} \tag{2}$$

where σ_o is the inert fracture stress.

The testing of fracture toughness is usually conducted under an ordinary laboratory condition of SCG. Yet even under this condition, if the crack size at the fracture, c_f, is used in the calculation, we can obtain the inherent fracture toughness (K_{IC}) from Eq. (1).[10,15] However, given the difficulty of determining c_f on the fractured surface, c_o is generally used in the calculation because it can be easily determined on fractured surfaces. Thus, the toughness value we obtained is not an inherent value but an apparent value that can be expressed by

$$K_{app} = \sigma_f Y c_o^{1/2} = K_{IC}\left(\frac{1}{1+\frac{\Delta c}{c_o}}\right)^{1/2} \tag{3}$$

Note that the fracture toughness depends on the ratio of crack extension to crack size.

The crack extension, Δc, depends on the SCG rate and the duration of the test. Meanwhile, the SCG rate depends on the environment (relative humidity), and the duration of the test time depends on the loading rate and the crack size. Thus, we may replace Δ_c/c_o in Eq. (3) by the function of c_o, $\dot{\sigma}$ (loading rate), and an appropriate parameter that reflects the effect of the environment. The function can be derived from the kinetics of SCG, which is frequently expressed by an empirical equation as follows:[14]

$$v = \frac{dc}{dt} = \alpha K_I^n \tag{4}$$

where α is a parameter that reflects the environment (relative humidity) and n is the SCG exponent. Following a procedure described in textbooks,[17] we obtained the following equation:

$$\sigma_f^{n+1} = k\dot{\sigma}\left(c_o^{\frac{2-n}{2}} - c_f^{\frac{2-n}{2}}\right) \tag{5}$$

where

$$k = \frac{2(n+1)}{n-2}\frac{1}{\alpha Y^n}$$

When c_f is appreciably larger than c_o, we can neglect the second term in the bracket of Eq. (5) to give

$$\sigma_f^{n+1} = k\dot{\sigma}c_o^{\frac{2-n}{2}} \tag{5'}$$

The combination of Eq. (1) and Eq. (5') yields

$$\frac{\Delta c}{c_o} = k'\alpha^{\frac{2}{n+1}}\dot{\sigma}^{\frac{-2}{n+1}}c_o^{\frac{-3}{n+1}} - 1 \tag{6}$$

where

$$k' = K_{IC}^2\left(\frac{n-2}{2(n+1)}\right)^{\frac{2}{n+1}}Y^{\frac{-2}{n+1}}$$

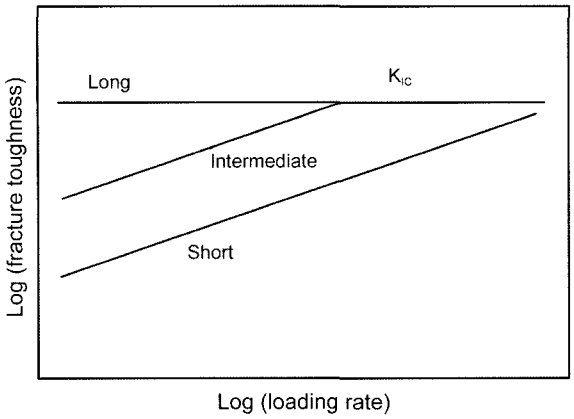

Fig. 4. Prediction of the change in the fracture toughness as a function of the loading rate for three different crack sizes in a logarithmic scale.

By inserting Eq. (6) into Eq. (3), we obtained the following equation:

$$K_{app} = k'' \alpha^{\frac{-1}{n+1}} \dot{\sigma}^{\frac{1}{n+1}} c_o^{\frac{3}{2(n+1)}} \tag{7}$$

where

$$k'' = \left(\frac{2(n+1)}{n-2}\right)^{\frac{1}{n+1}} Y^{\frac{1}{n+1}}$$

If c_f is not appreciably larger than c_o, the second term in the bracket of Eq. (5) cannot be neglected. In this case, no explicit function of K_{app} can be obtained. However, if c_f is close to c_o (that is, $\Delta c \approx 0$), K_{app} is also close to K_{IC}. At the extreme of $c_f = c_o$, K_{app} is equal to its corresponding inherent value, K_{IC}.

5. Discussion

Fig. 4 shows how the fracture toughness changes as a function of the loading rate at a given relative humidity in a logarithmic scale for three different crack sizes, which can be constructed from our theoretical analysis. If the crack size is relatively small, the fracture toughness increases as the loading rate increases, with a slope (in Fig. 4) given by $1/(n + 1)$ (Eq. (7)). However, if the crack size is large, $\Delta c/c_o$ in Eq. (6) can become close to zero (that is, $c_f \approx c_o$) even at a low loading rate. Thus, K_{app} is close to its inherent value (K_{IC}) even at the low loading rate and does not change with a further increase of the loading rate. When the crack size has an intermediate value, the fracture toughness increases until the loading rate increases to a certain value beyond which the toughness is close to K_{IC} and fails to change with the loading rate.

Relative humidity affects α in Eqs. (6) and (7) (α increases as the relative humidity increases). Thus, the relative humidity can also affect the fracture toughness. Because we had no expression of the relation between α and the relative humidity, we could not directly correlate the fracture toughness with the relative humidity. However, for a large crack size, we expect the toughness to have a value close to inherent value at a given loading rate, even at high humidity. Thus, the toughness does not change with humidity. In contrast, if the crack size is relatively small, the toughness increases as the relative humidity decreases. When a crack has an intermediate size, fracture toughness increases as the relative humidity decreases, until the toughness decreases to a certain value below which the toughness fails to change any more as the relative humidity decreases.

The above illustrations are consistent with the experimental results. The results show that fracture toughness by the SCF method increases as the crosshead rate increases, though the toughness eventually comes close to an inert value at the fastest crosshead rate in our experiments, that is, 2 mm/min. The toughness also increases as the relative humidity decreases until around 40%; below this level, the toughness values become close to the value of the inert toughness. With the SCF method, the way the fracture toughness changes in relation to the crosshead rate or the relative humidity might be attributable to the intermediate size of the cracks. In contrast, the toughness values obtained by the SEPB method and the SEVNB method, which are close to their corresponding inert values, do not change in relation to the crosshead rate or the relative humidity. These results can be attributed to the relatively long cracks in the specimens of the SEPB method or the SEVNB method.

Our results have an implication for dynamic fatigue testing. In dynamic fatigue testing, the strength of ceramics is measured at various loading rates, and the SCG exponent, n, is obtained by the slope of a log (strength) to log (loading rate) curve. An assumption that underlies this phenomenon is that c_f is appreciably larger than c_o. To reduce the strength variability, which originates from a distribution of the strength-determining critical flaws in the specimens, we may use cracked or notched specimens. However, our results imply that cracks or notches should be small enough to ensure that the assumption is valid at any loading rates. If cracks or notches are not sufficiently small, c_f can become close to c_o, especially at high loading rates, and the obtained SCG exponent may be erroneous.

We can highlight this phenomenon by comparing the SCG exponents obtained from the flexural strength data and the toughness data obtained by the SCF method. Because strength is linearly proportional to toughness (Eq. (1)), it does not make any difference whether SCG exponent is obtained from a log (strength) to log (loading rate) curve or a log (toughness) to log (loading rate) curve. Although the exponent obtained from the flexural strength data was 29.7, the exponent obtained by the SCF method from the toughness data was 36.1. That is, the exponent obtained by the SCF method from the toughness data was significantly larger than that obtained from the strength data. However, when we excluded the toughness at the loading rate of 2 mm/min, which is close to the value of its inert toughness

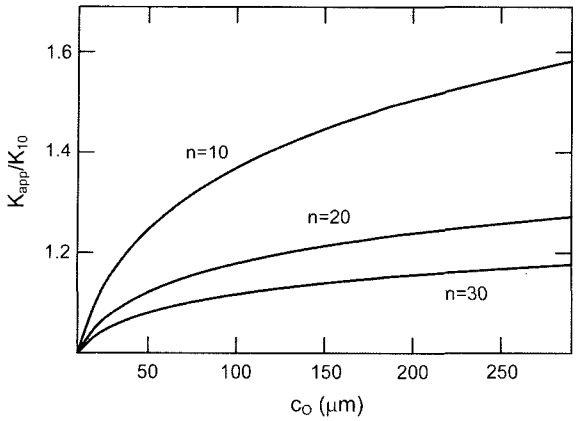

Fig. 5. Change in fracture toughness as a function of crack size at a given loading rate and humidity, which is predicted by Eq. (8). The toughness was normalized by a reference value, K_{10}, which represents the toughness at a crack size of 10 μm.

(Fig. 2), the exponent was 29.9, a value that agrees well with the exponent obtained from the flexural strength data. This result implies that we should take precautions obtaining the SCG exponent while testing cracked or notched specimens.

Finally, it is interesting to illustrate how the fracture toughness changes as a function of the crack size at a given loading rate and relative humidity. For the sake of our discussion, we can normalize Eq. (7) by using a value of the reference toughness for a specific crack size (say, 1 μm, 10 μm or whatever). This normalization gives

$$\frac{K_{app}}{K_{ref}} = \left(\frac{c_o}{c_{o,ref}}\right)^{\frac{3}{2(n+1)}} \tag{8}$$

We selected, for example, $c_{o,ref} = 10$ μm, and, in Fig. 5, we plotted Eq. (10) for $n = 10$, 20, and 30. We also assumed that the range of crack sizes given in the horizontal axis was sufficiently small to ensure that K_{app} is always smaller than the inherent toughness (K_{IC}) at a given loading rate and humidity.

Interestingly, our curves are similar to the well-known microstructure-induced increasing R-curves.[18,19] In our analysis, we assumed no microstructure-induced R-curve behavior. Thus, the fact that the fracture toughness increases as the crack size increases is due solely to the SCG effect. This phenomenon, in turn, implies that if the testing is not conducted under an inert condition the fracture toughness appears to increase as the crack size increases, even in materials that exhibit no microstructure-induced R-curve behavior. Indeed, Swab and Quinn observed that the toughness of fine-grained alumina, which exhibits no R-curve behavior, increases as the crack size increases.[15] Moreover, Fig. 5 shows that fracture toughness increases significantly in relation to the increasing crack size whenever n is small. Eq. (10), for example, predicts that a tenfold increase in the crack size (say, from 10 μm to 100 μm or from 100 μm to 1 mm) increases the toughness by as much as 40% for $n = 10$, 18% for $n = 20$, and 12% for $n = 30$.

5. Conclusion

When we used the SCF method, we experimentally showed that fracture toughness increases whenever the loading rate increases and whenever the relative humidity decreases. In contrast, when we used the SEPB method and the SEVNB method, we showed that fracture toughness shows no change with either the loading rate or the relative humidity. By considering crack size in our theoretical analysis of the way the loading rate and relative humidity affect fracture toughness, we attribute the different effects of the testing methods to the size of the cracks.

Acknowledgment

This work was supported by KRISS and the MOST of Korea through the National Research Laboratory Program. The authors thank Dr. H. M. Park at KRISS for helpful discussions.

REFERENCES

1. R. W. Davidge, J. R. McLaren, and B. Tappin, "Strength-Probability-Time (SPT) Relationships in Ceramics," *J. Mat. Sci.*, **8** 1699-705 (1973).
2. P. J. Dwivedi and D. J. Green, "Determination of Subcritical Crack Growth Parameters by In Situ Observation of Indentation Cracks," *J. Am. Ceram. Soc.*, **78** [8] 2122-28 (1995).
3. J. E. Ritter, "Engineering Design and Fatigue Failure of Brittle Materials," pp. 667-686 in Fracture mechanics of ceramics, Vol. 4 crack growth and microstructure, edited by R. C. Bradt, D. P. H. Hasselman, and F. F. Lange, Plenum Press, New York, 1978.
4. D. B. Marshall and B. R. Lawn, "Flaw Characteristics in Dynamic Fatigue : The Influence of Residual Contact Stress," *J. Am. Ceram. Soc.*, **63** 532-36 (1980).
5. K. Zeng, K. Breder, and D. Rowcliffe, "Comparison of Slow Crack Growth Behavior in Alumina and SiC-Whisker-Reinforced Alumina," *J. Am. Ceram. Soc.*, **76** [7] 1673-80 (1993).
6. C. C. McMahon, "Relative Humidity and Modulus of Rupture," *J. Am. Ceram. Soc.*, **58** [9] 873 (1979).
7. G. K. Bansal, W. H. Duckworth, and D. E. Niesz, "Strength-Size Relations in Ceramic Materials : Investigation of an Alumina Ceramic," *J. Am. Ceram. Soc.*, **59** [11-12] 472-78 (1976).
8. S. J. Cho, K. J. Yoon, J. J. Kim, and K. H. Kim, "Influence of Humidity on the Flexural Strength of Alumina," *J. Eur. Ceram. Soc.*, **20** 761-64 (2000).
9. J. Kubler, "Fracture Toughness of Ceramics Using the SEVNB Method; Round Robin," VAMAS Report No. 37, Swiss Federal Laboratories for Materials Testing and Research, Switzerland (1999).
10. J. K. Park, K. Yasuda, and Y. Matsuo, "Effect of Crosshead

Speed on the Fracture Toughness of Soda-Lime Glass, Al_2O_3, and Si_3N_4 Ceramics Determined by the Surface Crack in Flexure (SCF) Method," *J. Mat. Sci.*, **36** [9] 2335-42 (2001).

11. G. D. Quinn, J. J. Kubler, and R. J. Gettings, "Fracture Toughness of Advanced Ceramics by the Surface Crack in Flexure (SCF) Method : A VAMAS Round Robin," VAMAS Report No. 17, National Institute of Standards and Technology, Gaithersburg, MD, 1994.
12. T. Nose and T. Fujii, "Evaluation of Fracture Toughness for Ceramic Materials by a Single-Edge Precracked-Beam Method," *J. Am. Ceram. Soc.*, **71** [5] 328-33 (1988).
13. S. J. Cho, K. J. Yoon, Y. C. Lee, and M. C. Chu, "Effects of Environmental Temperature and Humidity on the Flexural Strength of Alumina and Measurement of Inert Strength," *Mater. Lett.*, **57** 2751-54 (2003).
14. Fine Ceramics : Determination of Fracture Toughness at Ambient Temperature by Single Edge Precracked Beam (SEPB) Method, ISO DIS 15732, International Standardization Organization, 2000.
15. J. J. Swab and G. D. Quinn, "Effect of Precrack "Halos" on Fracture Toughness Determination by the Surface Crack in Flexure Method," *J. Am. Ceram. Soc.*, **81** [9] 2261-68 (1998).
16. S. M. Wiederhorn, "Subcritical Crack Growth in Ceramics," in Fracture Mechanics of Ceramics, Vol. 2, pp. 613-46, Edited by R. C. Bradt, D. P. H. Hasselman, and F. F. Lange, Plenum Press, New York, 1974.
17. J. B. Wachtman, Mechanical Properties of Ceramics, Ch. 8., John Wiley & Sons, Inc., New York, 1996.
18. S. J. Bennison and B. R. Lawn, "Role of Interfacial Grain-bridging Sliding Friction in the Crack-Resistance and Strength Properties of Nontransforming Ceramics," *Acta Metall.*, **37** [10] 2659-71 (1989).
19. R. F. Cook, B. R. Lawn, and C. J. Fairbanks, "Microstructure-Strength Properties in Ceramics : I, Effect of Crack Size on Toughness," *J. Am. Ceram. Soc.*, **68** [11] 604-15 (1985).